

An optomechanical pressure sensor using multimode interference couplers with polymer waveguides on a thin p⁺-Si membrane

Dooyoung Hah ^{*}, Euisik Yoon, Songcheol Hong

Department of Electrical Engineering, Korea Advanced Institute of Science and Technology, 373-1 Kusong-dong, Yusong-gu, Taejeon, 305-338, South Korea

Accepted 14 September 1999

Abstract

We report a new optomechanical pressure sensor using multimode interference (MMI) couplers with polymer waveguides and a thin p⁺-Si membrane. We have simulated device characteristics by the normal mode theory and the mode propagation method applied to deflection and strain of the membrane. The optical waveguide is made of a single-mode, rib type of NOA73/PMMA/SiO₂ multi-layer system. The devices have been fabricated on the thin p⁺-Si membranes which are selectively etched using bulk micromachining. Device size is 0.4 mm (width) × 13 mm (length) and the total thickness of the membrane is 7 μm. The device characteristics are measured using a He–Ne laser (λ = 632.8 nm) as a light source. High sensitivity of 8.2 ppm/Pa has been obtained in the range of 100 kPa. © 2000 Elsevier Science S.A. All rights reserved.

Keywords: Optomechanical pressure sensor; Multimode interference couplers; p⁺-Si membrane; Polymer waveguides; Bulk micromachining

1. Introduction

Most semiconductor pressure sensors reported up to date have used the capacitive [1] or piezoresistive [2] mechanisms. Capacitive pressure sensors have shown good performance in terms of sensitivity while piezoresistive sensors have shown good linearity. However, both of sensing schemes are fatally sensitive when they are exposed to severe electromagnetic radiation. Recently, optomechanical pressure sensors have been studied as a good alternative, especially in electromagnetically active environments. There are several reports on optomechanical pressure sensors [3–9]. Brabander et al. [3] utilized an integrated optical ring resonator which measures strain by frequency changes, hence, it requires additional circuits for encoding. Kim and Neikirk [4] measured pressure by the reflectance changes of the Fabry–Perot cavity. In this approach, the thickness control of the device is very critical and complicated. Several research groups used Mach–Zehnder interferometers (MZIs) with Y-branches [5–9]. The Y-branches are typically lossy and long (> 1 cm) [5–9]. In these approaches, thick bulk-micromachined silicon membranes (> 60 μm) have been employed as

sensing diaphragms [5,7–9]; therefore, the device size should be large, at least 120 mm², for sufficient sensitivity.

In this paper, we propose a new optomechanical pressure sensor using multimode interference (MMI) couplers which provide lower loss and are much shorter than Y-branches. The proposed sensor also includes a thin p⁺-Si membrane which works as an etch-stop layer, resulting in a reduced device size. In the previous work [10] we reported the pressure sensor fabricated using a silica-based waveguide layers system as used by most of reported optomechanical pressure sensors. In this work, we have utilized a polymer-based waveguide layers system because the silica-based waveguide system is difficult to control stress, refractive index, and uniformity. By using the polymer-based waveguide system, we have achieved small residual stress, easy fabrication and low cost.

2. Operation mechanism

The schematic diagram of the proposed sensor is depicted in Fig. 1. It consists of two MMI couplers, two arms and a membrane. One arm (arm 1) is located on the center of the membrane and the other arm (arm 2) is located on the edge. An input MMI coupler has been designed to

^{*} Corresponding author. Tel.: +82-42-869-8049; fax: +82-42-869-8560; e-mail: hady@oerc.kaist.ac.kr

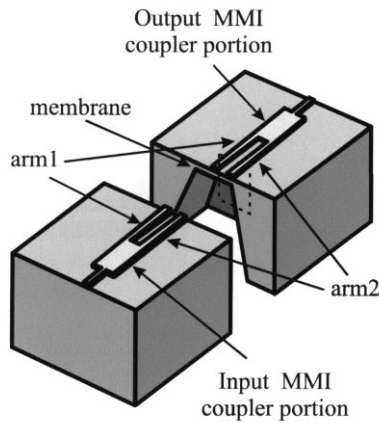
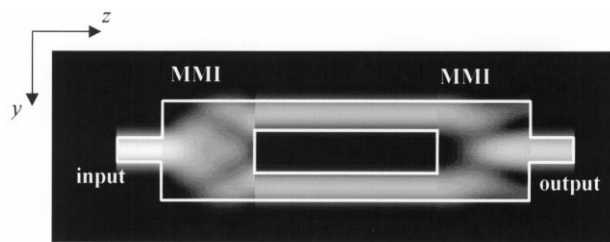


Fig. 1. Schematic cross-section of the proposed sensor. Arm 1 is located at the center of the membrane and arm 2 is located on the edge (not to scale).

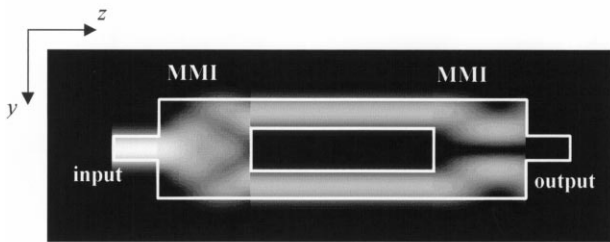
divide input light into two equal-power lights in the two arms [11]. When no pressure is applied to the membrane (Fig. 2(a)), the divided lights meet at the output MMI coupler in the same phase, so that they can be constructively interfered at the output MMI coupler. When the pressure is applied to the membrane (Fig. 2(b)), the strain induced in the membrane due to deflection causes the phase changes in the two arms by the following two mechanisms. One is the path length modulation and the other is the photoelastic effect which can be written as:

$$\Delta\left(\frac{1}{n_y^2}\right) = p_{yy}S_y + p_{yz}S_z \quad (1)$$

where n_y is refractive index, p_{yy} and p_{yz} are photoelastic coefficients, and S_y and S_z are strains [12]. As will be



(a)



(b)

Fig. 2. Simulated light propagation through the MMI couplers in the proposed sensor when (a) no pressure is applied and (b) pressure is applied (not to scale).

explained in Section 3.2, the strain and the amount of path changes are varied according to the location of the arm on the membrane. From these mechanisms, the output power of the output MMI coupler is varied by pressure change.

3. Design and simulation

3.1. Optical design

Waveguide layers are designed as a single-mode rib type consisting of NOA73/PMMA/SiO₂ multi-layers as shown in Fig. 3. NOA73 is commercially available optical adhesive. The advantages of this multi-layer waveguide system are ease of fabrication, low cost and relatively small residual stress. The thickness of the NOA73 core layer is 2.0 μm for single-mode operation at $\lambda = 632.8$ nm. The width and height of the rib are 5 and 0.15 μm, respectively. The thicknesses of the PMMA and the SiO₂ lower cladding layer are 2.0 and 0.2 μm, respectively, to prevent light leakage to the Si substrate. The refractive index of each layer is given in Fig. 3. The 3 dB dividing length of an MMI coupler, L_{3dB} , is shown in Fig. 4 and can be expressed as:

$$L_{3dB} \cong \frac{p}{2} \frac{n_f}{\lambda_0} \left(W_M + \frac{\lambda_0}{\pi} \frac{1}{\sqrt{n_f^2 - n_s^2}} \right)^2 \quad (2)$$

where λ_0 is wavelength and p is an odd number [11]. We must consider the two factors in the design of the MMI couplers. One is that L_{3dB} decreases as the width of the MMI coupler (W_M) decreases. The other factor is that the spacing between the two arms must be sufficient, so that the lights propagating through the arms do not couple to each other. The designed width (W_M) and L_{3dB} of MMI couplers are 20 μm and 2.5 mm, respectively, and the length of each arm is 8 mm. The total length of the device

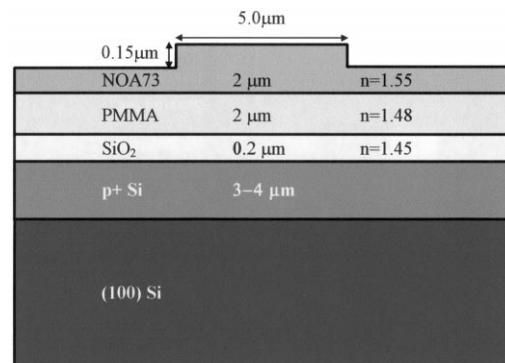


Fig. 3. Designed waveguide layer system (n is refractive index).

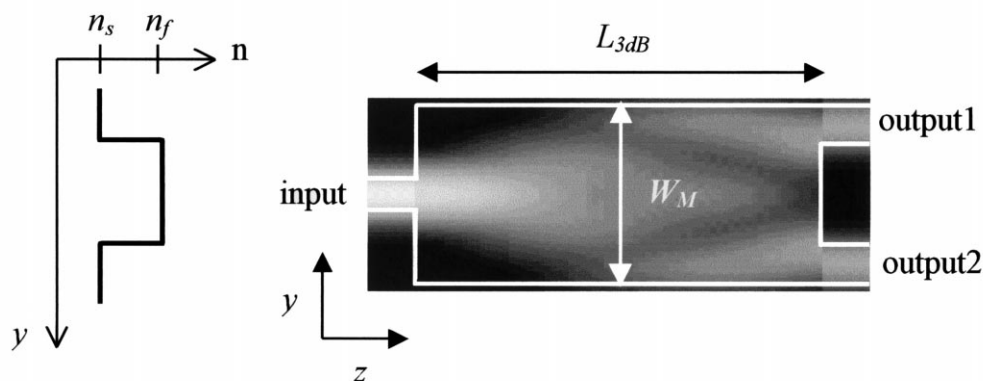


Fig. 4. Schematic diagram of the MMI coupler.

is 13 mm. This is much smaller than the dimension of the previous sensors using Y-branches (> 4 cm) [5–9].

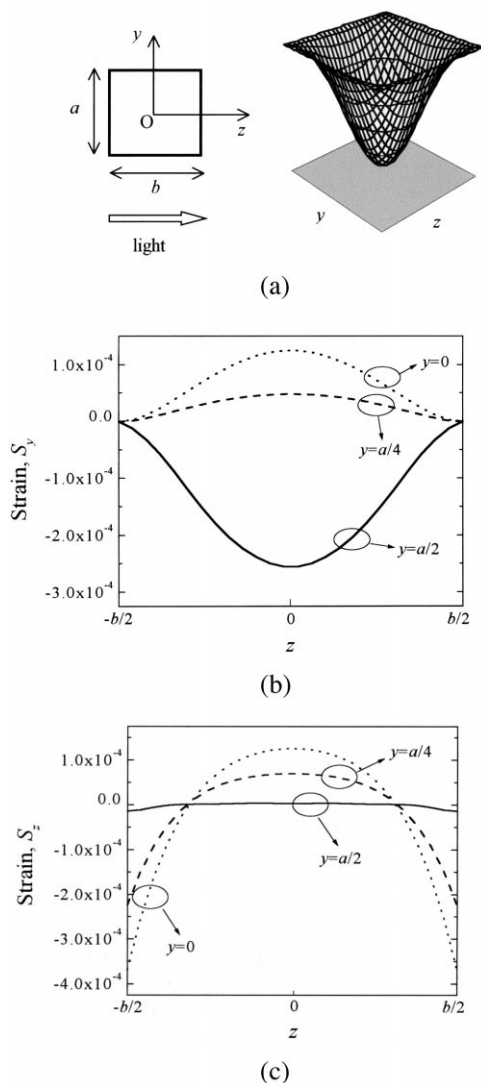


Fig. 5. (a) Calculated profile of diaphragm deflection, (b) simulated strains of y component and (c) simulated strains of z component of a membrane when pressure is applied.

3.2. Mechanical design

Since most polymer thin films are soft, they need supporting layers to form membranes with those films. We have chosen a p^+ -Si layer as the supporting layer. It is well-known that a heavily boron-doped ($> 7 \times 10^{19} \text{ cm}^{-3}$) silicon layer has a high etch selectivity in the anisotropic Si etchant, ethylenediamine pyrocatechol or EDP. By using this p^+ -Si layer, we can obtain a thin membrane with a well-controlled thickness. The thickness of the p^+ -Si layer is typically 3–4 μm and the area of the membranes have been designed from 0.4×0.4 to $1.0 \times 1.0 \text{ mm}^2$.

3.3. Simulation

Device simulation has been performed in the following two steps. First, the deflection and strain of the membrane are calculated as a function of pressure by an analytical method. Next, light propagation through the entire device is simulated by the normal mode theory (NMT) [13] as well as the mode propagation method (MPM) [11], using the strain and the amount of path change calculated in the previous step. From the NMT, we can obtain propagation constants and the guided mode profiles of a given layer structure. At the interface between two different waveguide structures, the mode conversion factor is calculated by the overlap integral of the mode profiles of the two structures by the MPM. If we assume that all membrane

Table 1
Parameter values used in simulation

Young's modulus	
E_{Si}	190 GPa
E_{NOA73}	2.5 GPa
E_{PMMA}	2.5 GPa
E_{SiO_2}	57 GPa
Photoelastic coefficients	
p_{yy}	0.05
p_{yz}	0.06

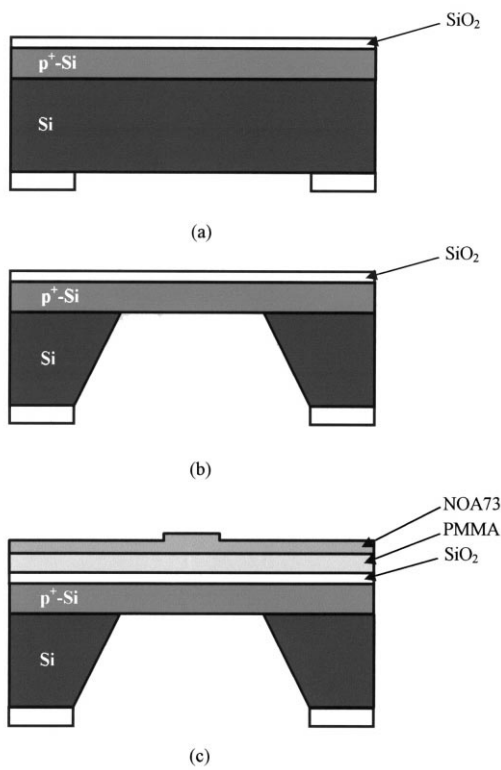


Fig. 6. Fabrication process of the proposed sensor: (a) p⁺ diffusion and thermal oxidation, (b) silicon bulk micromachining for p⁺-Si membrane formation, (c) definition of waveguide layers (not to scale).

edges are built-in, the deflection (w) is described by the superposition of the deflection of the simply supported

plate (w_0) and that of the plate by moments distributed along the edges ($w_{1,2}$) as follows:

$$w = w_0 + w_1 + w_2 \quad (3a)$$

$$w_0 = \frac{4qa^4}{\pi^5 D} \sum_{m=1,3,5,\dots}^{\infty} \frac{(-1)^{(m-1)/2}}{m^5} \cos \frac{m\pi y}{a} \times \left(1 - \frac{\alpha_m \tan h \alpha_m + 2}{2 \cos h \alpha_m} \cos h \frac{m\pi z}{a} + \frac{1}{2 \cos h \alpha_m} \frac{m\pi z}{a} \sin h \frac{m\pi z}{a} \right) \quad (3b)$$

$$w_1 = \frac{a^2}{2\pi^5 D} \sum_{m=1,3,5,\dots}^{\infty} E_m \frac{(-1)^{(m-1)/2}}{m^2 \cos h \alpha_m} \cos \frac{m\pi y}{a} \times \left(\frac{m\pi z}{a} \sin h \frac{m\pi z}{a} - \alpha_m \tan h \alpha_m \cos h \frac{m\pi z}{a} \right) \quad (3c)$$

$$w_2 = \frac{b^2}{2\pi^5 D} \sum_{m=1,3,5,\dots}^{\infty} F_m \frac{(-1)^{(m-1)/2}}{m^2 \cos h \beta_m} \cos \frac{m\pi z}{b} \times \left(\frac{m\pi y}{b} \sin h \frac{m\pi y}{b} - \beta_m \tan h \beta_m \cos h \frac{m\pi y}{b} \right) \quad (3d)$$

$$D = \frac{Eh^3}{12(1-\nu^2)}, \quad \alpha_m = \frac{m\pi b}{2a}, \quad \beta_m = \frac{m\pi a}{2b}$$

where h , E , and ν are thickness, Young's modulus, and Poisson's ratio of the membrane, respectively, and E_m and

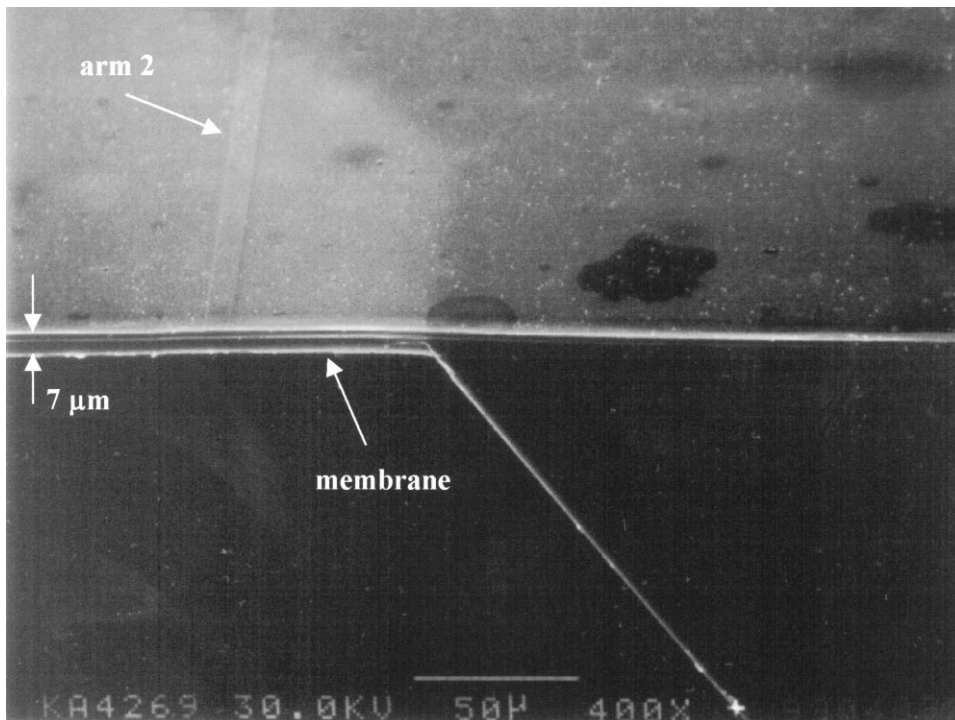


Fig. 7. A SEM picture of the fabricated sensor.

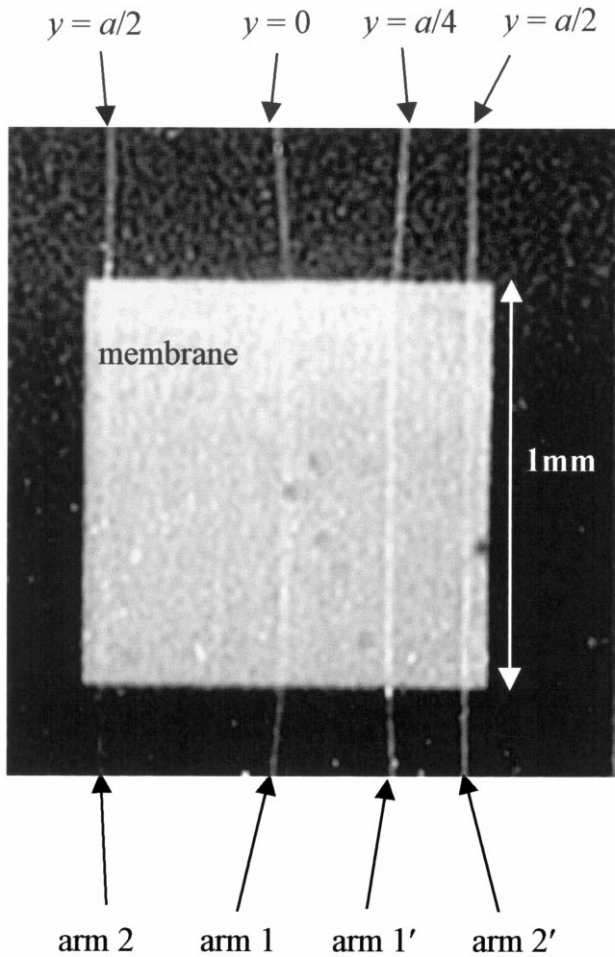


Fig. 8. A microscopic picture of the fabricated sensors from the top. Two devices on a membrane.

F_m are coefficients calculated from the boundary conditions [14]. a and b are the lateral extents of the membrane. The maximum strain $(S_{y,z})_{\max}$ is expressed as:

$$(S_y)_{\max} = \frac{h}{2} \frac{\partial^2 w}{\partial y^2} \quad (4)$$

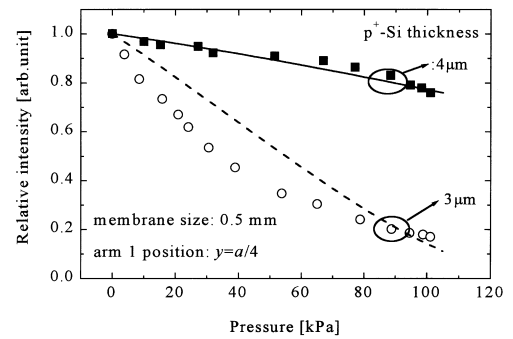
$$(S_z)_{\max} = \frac{h}{2} \frac{\partial^2 w}{\partial z^2} \quad (5)$$

Fig. 5(a) shows the calculated deflection profile. Fig. 5(b) and (c) show the calculated strain profiles along the z direction at different y locations when pressure is applied to the membrane. From these figures, we know that the y and z components of strain (S_y , S_z) have maximum difference when they are measured between the edge ($y = a/2$) and the center ($y = 0$) of the membrane along the z direction. Hence, the sensitivity of the sensor is expected to be maximum when the arm 1 is located at the center and the arm 2 on the edge of the membrane. The

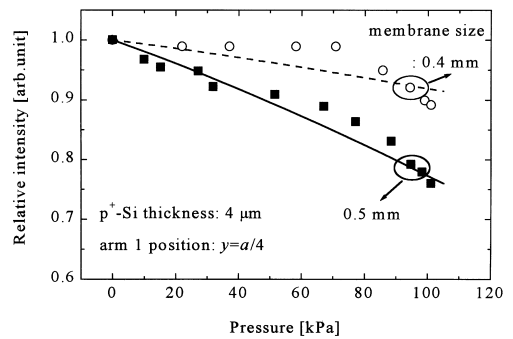
simulated light propagation through the device is drawn in Fig. 2 and the parameter values used in this simulation are summarized in Table 1. Young's modulus is quoted from Refs. [15,16] and photoelastic coefficients are fitted values from the measurement data.

4. Fabrication

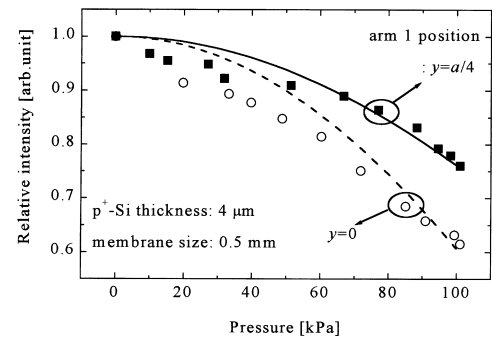
The sensor fabrication process is shown in Fig. 6. It starts with boron diffusion on the (100) Si substrate for 7 h at 1100°C in order to form a p^+ -Si etch-stop layer. The



(a)



(b)



(c)

Fig. 9. Measured (symbols) and simulated (lines) characteristics of the proposed sensors for (a) various p^+ -Si layer thicknesses (membrane size: 0.5 mm, arm 1: $y = a/4$), (b) various membrane sizes (p^+ -Si layer: 4 μm , arm 1: $y = a/4$), and (c) various arm 1 positions on the membrane (p^+ -Si layer: 4 μm , membrane size: 0.5 mm).

Table 2
Measured sensitivities of the proposed sensors in the range of 100 kPa

p ⁺ -Si thickness (μm)	Membrane size (mm)	Arm 1 position	Sensitivity (ppm/Pa)
3.0	0.5	$y = a/4$	8.22
4.0	1.0	$y = 0$	7.31
4.0	1.0	$y = a/4$	7.19
4.0	0.5	$y = 0$	3.82
4.0	0.5	$y = a/4$	2.38
4.0	0.4	$y = a/4$	1.07

first lower cladding layer (SiO_2) is formed by wet thermal oxidation for 1 h at 1000°C ($0.2 \mu\text{m}$). The backside SiO_2 layer formed from the thermal oxidation process is used as a mask for bulk Si etching. After opening the window of the backside SiO_2 in BOE, the anisotropic etching of the bulk Si is performed in EDP at 110°C for the membrane formation. The etching is stopped at the p⁺-Si layer. The composition of EDP is ethylenediamine:pyrocatechol: water = 350 ml:115 g:115 ml, and the etching rate is about $1 \mu\text{m}/\text{min}$ at that temperature. The PMMA layer ($2.0 \mu\text{m}$) is formed as a second lower cladding layer followed by the formation of the NOA73 core layer ($2.0 \mu\text{m}$) by spin coating and curing. The rib is formed by dry etching in RIE with O_2 gas. Fig. 7 shows the SEM picture of the fabricated device. The image shows the dotted box indicated in Fig. 1. Fig. 8 shows the top view of two devices on one membrane. Arm 1 of one sensor is at the center of the membrane ($y = 0$) and arm 1 of the other sensor is at $y = a/4$ position of the membrane. Total thickness of the membrane is $7 \mu\text{m}$. The root-mean-square roughness of p⁺-Si surface is about 10 nm (measured by an atomic force microscope), which corresponds to about 1/60 of the wavelength of the He–Ne laser. This will not significantly affect the optical performance.

5. Results

A He–Ne laser ($\lambda = 632.8 \text{ nm}$) light is introduced to the sensor through a lens and output light power is measured with a photodetector. Fig. 9 shows the measured (symbols) and simulated (lines) characteristics of the fabricated sensors with various membrane dimensions. From Fig. 9(a) and (b), it is shown that thinner and larger membranes are more sensitive. Fig. 9(c) confirms that sensor with the arm 1 at the center of the membrane ($y = 0$) is more sensitive than that with the arm 1 at $y = a/4$ as expected from the simulation. The difference between measured and simulated characteristics may be caused by the arm position variation due to the tolerance of front–back alignment. Table 2 summarizes measured sensitivities of the fabricated sensors. Measured sensitivities are from 1.1 to 8.2 ppm/Pa in the range of 100 kPa.

These are much higher than those of the capacitive pressure sensors which are typically $\sim 1 \text{ ppm}/\text{Pa}$ [1].

6. Conclusions

A new optomechanical pressure sensor using MMI couplers and polymer waveguides has been presented. By using MMI couplers and thin p⁺-Si membranes, we have achieved the device size as small as 0.4 mm (width) \times 13 mm (length). The size is reduced by ~ 20 times, compared to the previously reported optomechanical pressure sensors, which was 3 mm (width) \times 40 mm (length) [6–9]. The membrane size was 0.4 mm (width) \times 0.4 mm (length) \times $7 \mu\text{m}$ (thickness). We have obtained low-residual-stress waveguide layers by using polymer-based waveguide system. With this waveguide system, we have fabricated the sensor easily with low cost. To optimize the sensor characteristics, analysis and simulations on the photoelastic effect and path length modulation have been performed by using the normal mode theory and the mode propagation method. The sensor has been fabricated by means of bulk micromachining. Characteristics of the sensor have been measured with a He–Ne laser. The measured sensitivities were from 1.1 to 8.2 ppm/Pa in the range of 100 kPa. These are comparable to that of the reported optomechanical pressure sensor ($12.5 \text{ ppm}/\text{Pa}$) in the same range [17].

Acknowledgements

This work is partially supported by the Ministry of Information and Communication and by the Korea Science and Engineering Foundation under the contract OERC-1997G0202. The authors would like to thank Mr. E. Park and J. Park for their help in device fabrication.

References

- [1] J.T. Kung, H. Lee, An integrated air-gap-capacitor pressure sensor and digital readout with sub-100 attofarad resolution, *IEEE J. Microelectromech. Syst.* 1 (1992) 121–128.
- [2] B. Folkmer, P. Steiner, W. Lang, A pressure sensor based on a nitride membrane using single-crystalline piezoresistors, *Sensors and Actuators A* 54 (1996) 488–492.
- [3] G.N. Brabander, J.T. Boyd, G. Beheim, Integrated optical ring resonator with micromechanical diaphragm for pressure sensing, *IEEE Photon. Technol. Lett.* 6 (1994) 671–673.
- [4] Y. Kim, D.P. Neikirk, Micromachined Fabry–Perot cavity pressure transducer, *IEEE Photon. Technol. Lett.* 7 (1995) 1471–1473.
- [5] D. Peters, K. Fischer, J. Müller, Integrated optics based on silicon oxynitride thin films deposited on silicon substrates for sensor applications, *Sensors and Actuators A* 25–27 (1991) 425–431.

- [6] C. Wagner, J. Frankenberger, D.P. Deimel, Optical pressure sensor based on a Mach–Zehnder interferometer integrated with a lateral a-Si:H p-i-n photodiode, *IEEE Photon. Technol. Lett.* 5 (1993) 1257–1259.
- [7] K. Fischer, J. Müller, R. Hoffmann, F. Wasse, D. Salle, Elasto-optical properties of SiON layers in an integrated optical interferometer used as a pressure sensor, *J. Lightwave Technol.* 12 (1994) 163–169.
- [8] K. Hoppe, L.U.A. Andersen, S. Bouwstra, Integrated Mach–Zehnder interferometer pressure transducer, *Proc. 8th Int. Conf. Solid-state Sensors and Actuators, and Eurosensors IX, Stockholm, Sweden, 25–29 June, 1995*, pp. 590–591.
- [9] K. Benaissa, A. Nathan, IC compatible optomechanical pressure sensors using Mach–Zehnder interferometry, *IEEE Trans. Electron Devices* 43 (1996) 1571–1582.
- [10] D. Hah, E. Yoon, S. Hong, An optomechanical pressure sensor using multimode interference couplers, *Japanese Journal of Applied Physics* 38 (1999) 2664–2668.
- [11] L.B. Soldano, E.C.M. Pennings, Optical multi-mode interference devices based on self-imaging: principles and applications, *J. Lightwave Technol.* 13 (1995) 615–627.
- [12] A. Yariv, P. Yeh, *Optical Waves in Crystals*, Wiley, New York, 1983.
- [13] H. Ribot, P. Sansonetti, A. Carencio, Improved design for the monolithic integration of a laser and an optical waveguide coupled by an evanescent field, *IEEE J. Quantum Electron.* 26 (1990) 1930–1941.
- [14] S. Timoshenko, S. Woinosky-Krieger, *Theory of Plates and Shells*, McGraw-Hill, New York, 1959.
- [15] M. James, *Physical Properties of Polymers Handbook*, Woodbury, New York, 1996.
- [16] K.E. Petersen, Silicon as a mechanical material, *Proc. IEEE* 70 (1982) 420–457.
- [17] M. Ohkawa, M. Izutsu, T. Sueta, Integrated optic pressure sensor on silicon substrate, *Appl. Opt.* 28 (1989) 5153–5157.

Dooyoung Hah was born in Seoul, Korea in 1972. He received his BS and MS degrees in Electrical Engineering from the Korea Advanced Institute of Science and Technology (KAIST) in 1994 and 1996, respectively. He is currently working toward the PhD degree in Electrical Engineering at the KAIST. His research interests are in optomechanical microsensors and RF micromachined circuits.

Euisik Yoon was born in Seoul, Korea. He received the BS and MS degrees in Electronics Engineering from Seoul National University in 1982 and 1984, respectively, and PhD degree in Electrical Engineering from the University of Michigan, Ann Arbor, in 1990. From 1990 to 1994, he was with the Fairchild Research Center of the National Semiconductor, Santa Clara, CA, where he was engaged in researches on deep submicron CMOS integration and advanced gate dielectrics. From 1994 to 1996, he was a Member of Technical Staff at Silicon Graphics, Mountain View, CA, working on the design of the MIPS microprocessor R4300i and the RCP 3-D graphic coprocessor. In 1996, he joined the Department of Electrical Engineering at the KAIST, Taejeon, Korea, where he is currently an assistant professor. Currently, he serves as a technical advisory board member of Sandcraft, Santa Clara, CA. His present research interests are in microsensors, integrated microsystems, and VLSI circuit design.

Songcheol Hong received the BS and MS degrees in Electronics Engineering from Seoul National University in 1982 and 1984, respectively, and the PhD degrees in Electrical Engineering and Computer Science from the University of Michigan in 1989. He is currently a Professor in the Department of Electrical Engineering at the KAIST. He has been interested in monolithic microwave integrated circuits (MMIC) and novel quantum devices. Currently, active research areas include solid state power amplifiers, large signal models for microwave devices, quantum dot and well applications. He is a member of IEEE and KITE.